Am J Transl Res 2024;16(2):690-699
www.ajtr.org /ISSN:1943-8141/AJTR0154692

Brief Communication

Complex phenotypic heterogeneity of combined hepatocellular-cholangiocarcinoma with a homogenous *TERT* promoter mutation

Sumie Ohni[1], Hiromi Yamaguchi[2], Yukari Hirotani[1], Yoko Nakanishi[1], Yutaka Midorikawa[3], Masahiko Sugitani[4], Tomohiro Nakayama[5], Makoto Makishima[2], Mariko Esumi[2]

[1]Division of Oncologic Pathology, Department of Pathology and Microbiology, Nihon University School of Medicine, Tokyo, Japan; [2]Division of Biochemistry, Department of Biomedical Sciences, Nihon University School of Medicine, Tokyo, Japan; [3]Department of Surgery, Nihon University School of Medicine, Tokyo, Japan; [4]Division of Human Pathology, Department of Pathology and Microbiology, Nihon University School of Medicine, Tokyo, Japan; [5]Division of Clinical Laboratory Medicine, Department of Pathology and Microbiology, Nihon University School of Medicine, Tokyo, Japan

Received November 30, 2023; Accepted February 18, 2024; Epub February 25, 2024; Published February 28, 2024

Abstract: To clarify the mechanism underlying the development and poor prognosis of combined hepatocellular-cholangiocarcinoma (cHCC-CCA), we characterized liver cancer driver mutations and poor prognostic markers in both the HCC and intrahepatic CCA (iCCA) components of a cHCC-CCA tumor. The telomerase reverse transcriptase (*TERT)* promoter mutation C228T was quantified by digital polymerase chain reaction using DNA from multiple microdissected cancer components of a single cHCC-CCA nodule. The protein expression of cancer-related markers, including TERT, was examined by serial thin-section immunohistochemistry and double-staining immunofluorescence. *TERT* promoter mutation and TERT protein expression were detected in all cancer components but not in noncancer regions. *TERT* promoter mutation frequencies were similar among components; those of TERT protein-positive cancer cells were higher in iCCA and mixed components than in HCC. The frequencies of Ki67- and p53-positive cells were similarly higher in iCCA and mixed components than in HCC. However, double-positive cells for the three proteins were unexpectedly rare; single-positive cells dominated, indicating phenotypic microheterogeneity in cancer cells within a component. Interestingly, HCC and CCA marker protein immunohistochemistry suggested dedifferentiation of HCC and transdifferentiation from HCC to iCCA in HCC and iCCA components, respectively. Such phenotypic intercomponent heterogeneity and intracomponent microheterogeneity were detected in a tumor nodule of cHCC-CCA uniformly carrying the early HCC driver mutation. Moreover, poor prognostic markers were randomly expressed without a regular pattern, consistent with the poor prognosis.

Keywords: Combined hepatocellular-cholangiocarcinoma, *TERT* promoter mutation, digital PCR, TERT protein, Ki67, p53, immunohistochemistry, dedifferentiation, transdifferentiation, phenotypic heterogeneity

Introduction

Combined hepatocellular-cholangiocarcinoma (cHCC-CCA) is a rare tumor that accounts for 2% to 5% of primary liver cancers [1]; the actual incidence is likely higher due to underestimation of cHCC-CCA without biopsy [2]. Regardless, this tumor is aggressive and has a poor prognosis; in fact, its prognosis is worse than that of HCC and similar to that of intrahepatic cholangiocarcinoma (iCCA) [1, 2]. To understand the genesis of characteristic cHCC-CCA and identify significant clinical indicators, it is necessary to thoroughly investigate biologic behavior, such as the simultaneous development of two different tumors and aggressive progression. Regarding genesis, there are two theories involved in the synchronous development of the HCC and iCCA components of cHCC-CCA: multicentric origin and monoclonal origin. Current studies on sequence-based mutational profiles of individual cancer components of cHCC-CCA have shown that most cases, especially cHCC-CCA defined according to international consen-

https://doi.org/10.62347/CQJW7490

sus and the World Health Organization (WHO) [3, 4], are of monoclonal origin [5-7]. Monoclonal origin includes two scenarios: hepatic progenitor cell origin [5] and transdifferentiation of HCC to iCCA [6, 8]. Indeed, we demonstrated the latter, i.e., transdifferentiation of partial HCC to iCCA, using clinical samples obtained from a case of metachronous liver cancer development from HCC to cHCC-CCA over a three-year interval [8]. Although the mechanism of transdifferentiation remains unclear, the process itself or its environmental background could be factors leading to cancer progression with poor prognosis.

With respect to aggressive progression, three cancer-related factors were investigated in this study: *telomerase reverse transcriptase* (*TERT*) promoter mutation, TERT protein expression, and Ki67 protein and p53 protein expression in multiple components of a cHCC-CCA tumor. TERT reactivation occurs in most cancers and contributes to cancer formation and progression through telomere extension. *TERT* promoter mutation is key for many regulatory mechanisms involved in telomerase reactivation [9] and is closely associated with poor prognosis in terms of both disease-free survival and overall survival in HCC [10, 11]. Overexpression of Ki67 and p53 is also a cancer-associated phenotype that plays a role in the development and progression of cancers, including HCC. Ki67 is a proliferation marker widely employed for human tumor diagnostics. p53 is also frequently overexpressed in human tumors, including HCC. In general, immunohistochemistry (IHC)-has shown that p53 overexpression correlates with *p53* gene mutations in HCC patients (82.9% positive in mutant-p53 HCC), and *p53* genetic alterations are associated with aggressive malignant behavior and poor survival in HCC [12]. Although the above three proteins are related to cancer malignancy, the positive expression rate of these malignant markers in multiple cancer components of cHCC-CCA is unclear, and it is unknown whether their expression occurs in the same cancer cell. In this study, we examined the correlation of *TERT* promoter mutation frequency and TERT protein expression in multiple components of a single tumor nodule of cHCC-CCA and the relationship between the expression levels of the proteins TERT, Ki67, and p53. The findings obtained are helpful for understanding the biological behaviors of these cancer cells in relation to tumor development and progression.

Materials and methods

The patient in this case was male, 73 years old, and positive for anti-hepatitis C virus antibody. He underwent partial liver resection (5×3.5×3.5 cm) as curative treatment for a liver tumor (1.5×1.5×1.2 cm) in liver segment 8 (**Figure 1A**). Formalin-fixed, paraffin-embedded (FFPE) liver tissue blocks were prepared from the resected liver: #1, #2a, #2b, #3 and #4 (**Figure 1A**). The tumor was nodular-type and milky white; it was histologically diagnosed as cHCC-CCA. This study was approved by the Ethics Committee of Nihon University School of Medicine (approval no. 237-1). Informed consent was obtained from the patient prior to the start of the study. Detailed materials and methods such as liver specimens, DNA extraction, digital polymerase chain reaction (dPCR) of the TERT promoter mutation C228T, immunohistochemistry, immunofluorescence double staining for TERT/Ki67 and TERT/p53 and statistical analysis are described in Supplementary Materials (Materials and methods).

Results

Histological and immunohistochemical findings for cHCC-CCA

A single tumor nodule of cHCC-CCA was regionally separated histologically (**Figure 1A**). The HCC component was major and observed in blocks #2a, #2b, #3 and #4. The iCCA component was minor and observed in blocks #2b and #3. A component with a mixture of HCC and iCCA was also observed in blocks #2b and #3 in the middle of the tumor nodule (mixed HCC-iCCA) (**Figure 1A**). These components shown by hematoxylin and eosin (H&E) staining were confirmed by IHC for HCC (HepPar-1) and CCA (CK7, CK19, CA19-9) markers (**Figure 1B**). Interestingly, the HCC component occasionally contained HepPar-1-negative HCC cells (**Figure 1B**, lower), whereas HepPar-1 was specific for all hepatocytes in the noncancer region and HCC (**Figure 1B**, upper). This HCC component was also negative for CK7 (**Figure 1B**, lower). In contrast, the iCCA component occasionally contained rare iCCA cells positive for HepPar-1 (**Figure 1B**, lower). Thus, a variety of cancer cells were observed as minor components with

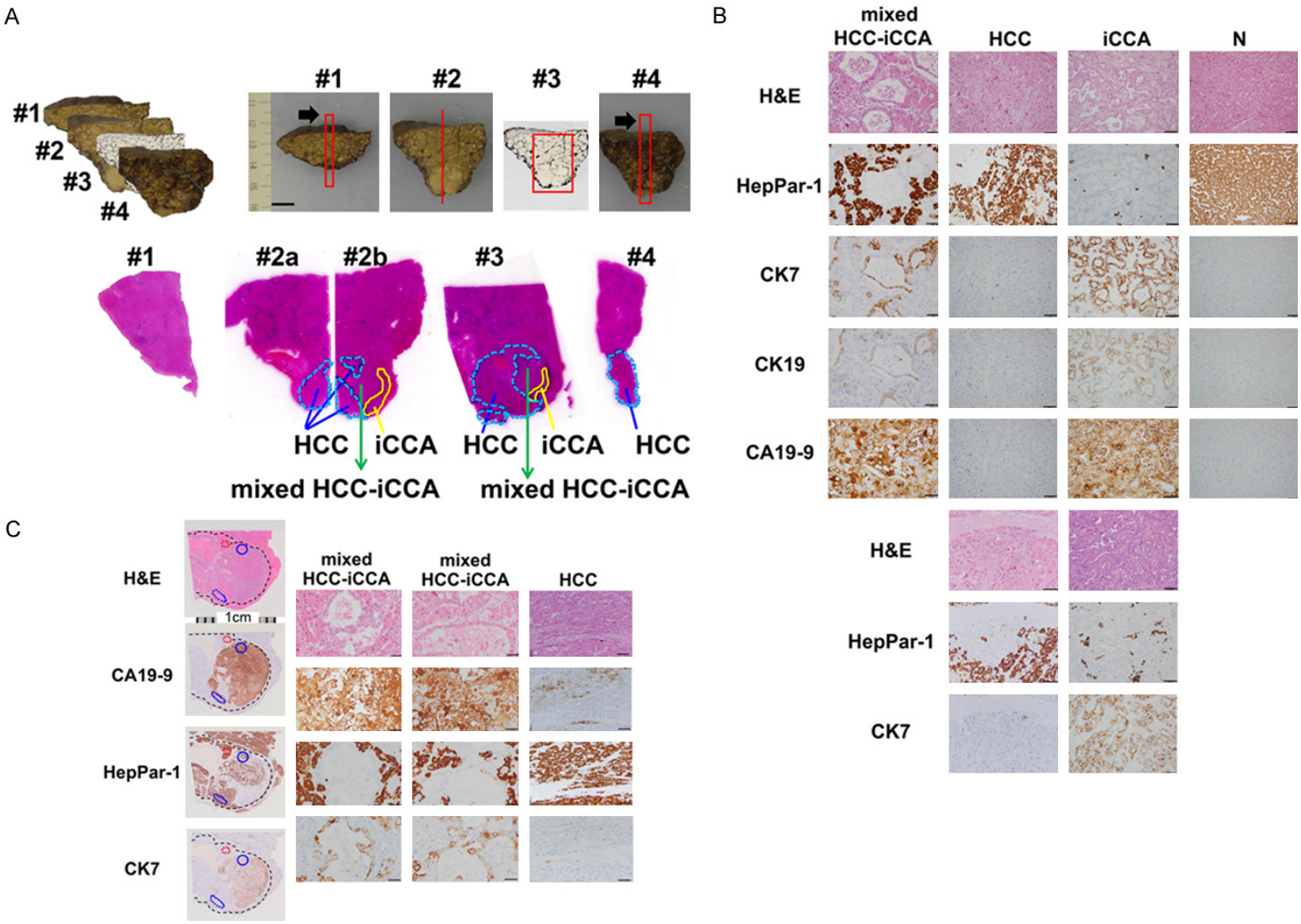

Figure 1. Gross and histopathologic findings of cHCC-CCA. (A) Gross cross-sections and histologic specimens of a curatively resected liver. The liver cancer cHCC-CCA was observed in sections #2, #3 and #4. Red indicates the cutting lines for the specimens. The block arrows in #1 and #4 indicate the direction of thin slice sections. The bar indicates 10 mm. Histological macrofeatures of HCC (blue) and iCCA (yellow) components, including mixed HCC-iCCA components (green), are shown in each thin slice section stained with H&E. (B) Representative IHC images of cHCC-CCA. Serial thin sections of the #2b tissue shown in (A) were subjected to H&E

staining and IHC staining for HepPar-1, CK7, CK19 and CA19-9. Representative images of four regions, mixed HCC-iCCA, HCC, iCCA and nontumorous liver (N), are shown. Bars indicate 50 μm. Particular IHC images of HCC and iCCA components are shown in the lower panel. HCC negative for HepPar-1 and CK7; iCCA cells positive for HepPar-1 and CK7. Bars indicate 100 μm. (C) Representative IHC images of HCC cells positive for CA19-9 in the mixed HCC-iCCA component (blue lines). High-magnification images are shown in the left (blue solid line) and middle (blue dotted line) panels (bar, 50 μm), and CA19-9(+)/HepPar-1(+)/CK7(-) HCC cells in areas of the HCC components (red dotted line) are shown by high magnification in the right panel (bar, 100 μm). Black dotted lines indicate a border between cancer and noncancerous regions.

dedifferentiated and transdifferentiated statuses. Second, CA19-9 was not only specific for iCCA but also positive in the iCCA-containing stroma (**Figure 1B**, upper). In particular, HCC adjacent to iCCA in the mixed HCC-iCCA region was strongly positive for CA19-9 (**Figure 1C**, for example, blue-marked areas-upper and lower-shown in the left and middle panels by high magnification, respectively), whereas most of the HCC component was negative for this marker (**Figure 1B** and **1C**). However, the HCC component contained rare HCC cells positive for CA19-9 (**Figure 1C**, a red-dotted area shown in the right panel by high magnification).

Frequency of the TERT promoter mutation C228T in multiple components of cHCC-CCA

The *TERT* promoter mutation is one of the driver mutations of HCC, distinct from iCCA [13, 14]. We found the monoclonal origin of cHCC-CCA using mutational profiles including the *TERT* promoter mutation C228T [8]. To examine the clonality and heterogeneity of cHCC-CCA, the mutation frequency of the *TERT* promoter mutation C228T was determined in multiple components of cHCC-CCA. Digital PCR for the *TERT* promoter mutation C228T was performed using DNA extracted from the whole tumor nodule (mixture of HCC and iCCA), three HCC components, an iCCA component, and two noncancer regions (N) in four independent experiments: Exp. 1, Exp. 2, Exp. 3 and Exp. 4 (**Figure 2A**). The mutation was detected in all tumor samples (**Figure 2B**); the mutation frequency was 19.3% to 34.9% in the HCC components, 36.2% in the iCCA component and 33.1% in the mixture (HCC, iCCA) (**Figure 2A**). Thus, in the present case of cHCC-CCA, all cancer components were positive for the examined *TERT* promoter mutation, with small variation in frequency, which was probably due to the varied stromal content within the microdissected components. The origin of HCC and iCCA might be the same, as shown in most cases of cHCC-CCA [5-8]. The liver cirrhotic lesions (the N1, N2) mostly showed no mutations in this case (**Figure 2**).

Protein expression of TERT, Ki67, and p53 in multiple components of cHCC-CCA

The *TERT* promoter mutation C228T elevates the level of *TERT* mRNA by creating the ETS active element sequence for the transcription factor GABP. To examine TERT expression at the protein level, we performed IHC (**Figure 3A**). TERT protein expression was positive in the nuclei of cancer cells but not all cells; the positive rate varied from 10% to 20% in each cancer component (**Figure 3B**). Noncancer regions were mostly negative for the TERT protein (**Figure 3B**). Thus, not all cancer cells carrying the *TERT* promoter mutation were positive for the TERT protein in our IHC system.

To examine the relationship of TERT-positive cells with markers of a poor prognosis, the proteins Ki67 and p53, we performed IHC using serial thin sections (**Figure 3C**). The Ki67 and p53 proteins were positive in the nuclei of cancer cells, and the proportion of positive cells was different in different components of cancer. HCC components had lower positive rates for both markers than iCCA ($P<0.01$, $P<0.001$ Mann-Whitney *U* test), but the positivity rates for two markers were similar within each cancer component (**Figure 3D**). Moreover, the frequency of cancer cells double-positive for Ki67 and p53 (KI67+/p53+) in each cancer component was unexpectedly low, at only 9.1%-24.5% of any positive cancer cell type (**Figure 3E**). In addition, the distribution of three types of cancer cells (Ki67+, p53+ and Ki67+/p53+) between HCC and iCCA components significantly differed ($P<0.05$, chi-square test), with Ki67+/p53+ cancer cells having a significantly higher rate in iCCA than in HCC ($P<0.01$, Mann-Whitney *U* test) (**Figure 3E**).

Relationship of TERT-positive cells with Ki67-positive and p53-positive cells

To precisely determine the relationship of TERT-positive cells to Ki67-positive cells or p53-positive cells, immunofluorescence double staining for TERT/Ki67 and TERT/p53 was performed in

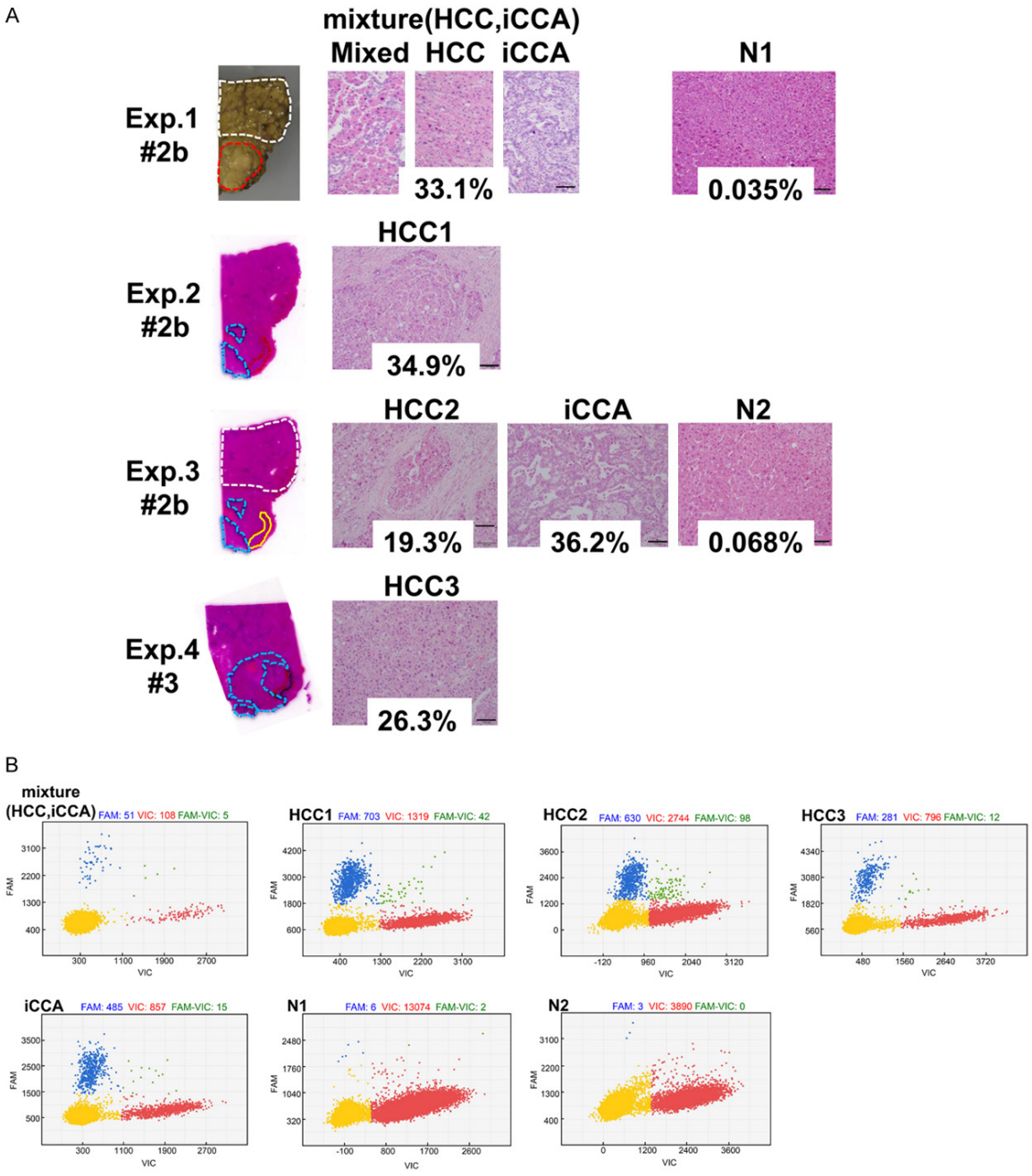

Figure 2. Frequency of the *TERT* promoter mutation C228T determined by dPCR. (A) Macroscopic and representative histologic images of seven liver tissue samples used for DNA extraction. Sampling areas are shown by colored dotted lines in four experiments using sections #2b and #3. In Exp. 1, cHCC-CCA containing components of mixed HCC-iCCA, HCC and iCCA (mixture in red) and noncancerous lesions (N1 in white) were macroscopically dissected from #2b tissue thin sections. In Exp. 2, the HCC component was laser-capture microdissected (HCC1 in blue). In Exp. 3, components of HCC (HCC2 in blue), iCCA (iCCA in yellow) and noncancerous lesions (N2 in white) were microscopically or macroscopically dissected from #2b. In Exp. 4, the HCC component was laser-capture microdissected from #3 (HCC3 in blue). The frequency of the *TERT* promoter mutation C228T determined by dPCR is shown under each panel. Bars indicate 100 μm. (B) Scatter plots of dPCR results for the C228T *TERT* promoter mutation. The seven DNA samples shown in (A) were subjected to dPCR. Blue (FAM), mutant allele; red (VIC), wild-type allele; green (FAM-VIC), both alleles; yellow, undetermined.

the mixed HCC-iCCA component (**Figure 4A**). TERT+/Ki67+ double-positive cells comprised 9.7% of any positive cell type, and TERT+/p53+ double-positive cells comprised 13.3%; the frequency was similarly low and not significantly different between the two (P=0.658, chi-square

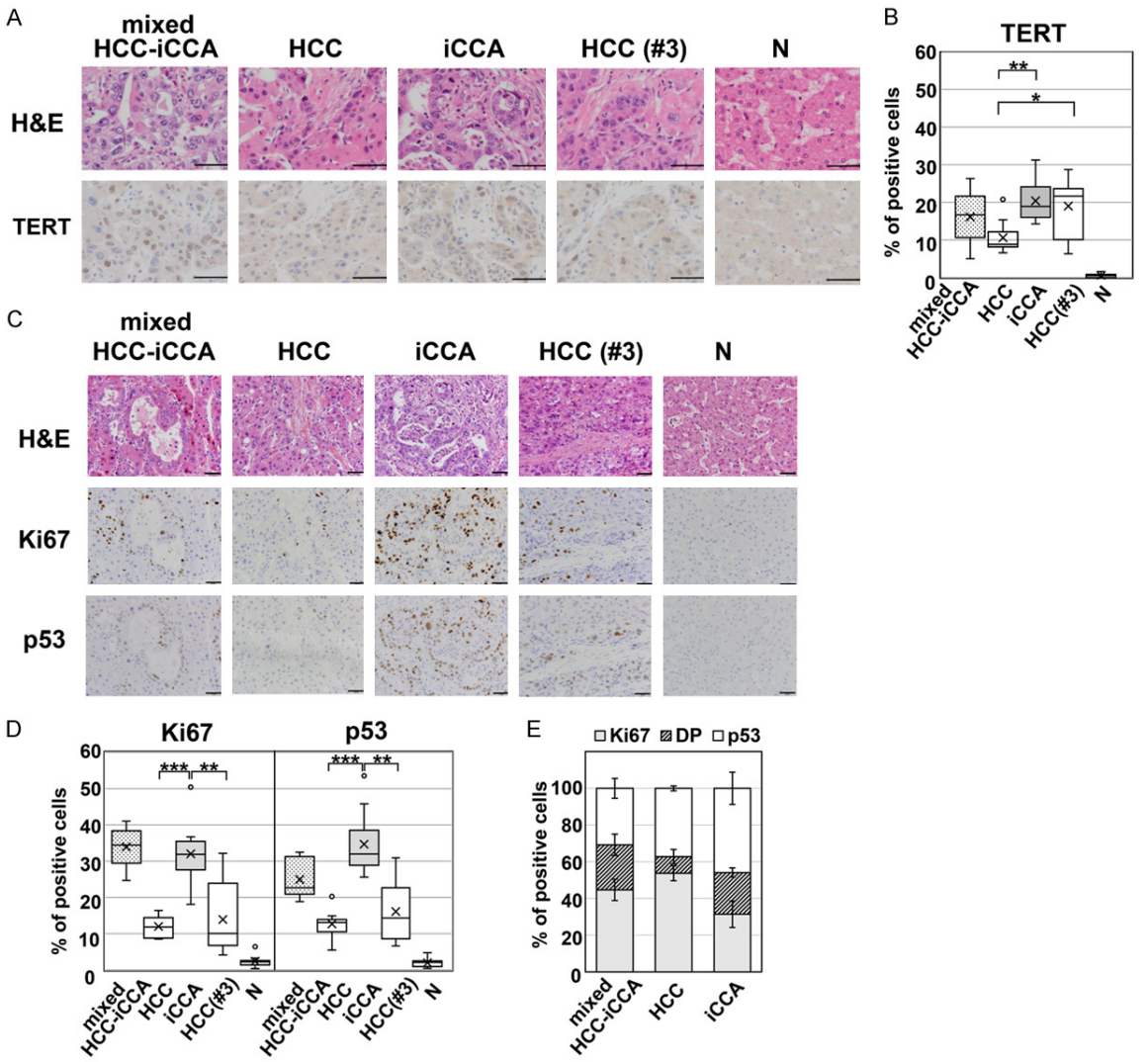

Figure 3. IHC of TERT, Ki67 and p53 proteins in various components of cHCC-CCA. A. Representative images of serial thin sections from #2b and #3 with H&E staining and IHC for TERT. Bars indicate 50 μm. B. Frequency of cells positive for TERT protein in mixed HCC-iCCA, HCC, iCCA, HCC (#3) and N. Only cancer components of HCC, iCCA and HCC (#3) were subjected to statistical analysis (*, *P<0.05*; **, *P<0.01* by Mann-Whitney *U* test). C. Representative images of serial thin sections from #2b and #3 with H&E staining and IHC for Ki67 and p53. Bars indicate 50 μm. D. Frequency of cells positive for Ki67 and p53 in mixed HCC-iCCA, HCC, iCCA, HCC (#3) and N. Only cancer components of HCC, iCCA and HCC (#3) were subjected to statistical analysis (**, *P<0.01*; ***, *P<0.001* by Mann-Whitney *U* test). E. Distribution of three types of cancer cells (Ki67+, p53+, Ki67+/p53+) in mixed HCC-iCCA, HCC and iCCA components. DP, double-positive cells (Ki67+/p53+).

test) (**Figure 4B**). Positive cytoplasmic staining of TERT was demonstrated by immunofluorescence staining (**Figure 4A**), and the cytoplasmic TERT staining rate was significantly lower among TERT+/Ki67+ double-positive cells than among TERT+ single-positive cells ($P<0.05$, Kruskal-Wallis test) (**Figure 4C**).

Discussion

We demonstrated herein that the TERT protein is expressed in all cancer components (HCC, iCCA and mixed HCC-iCCA) existing within a tumor nodule of cHCC-CCA carrying a promoter mutation, but not in noncancer regions without mutation. The similar mutation frequency of early HCC-specific driver genes in all cancer components suggests the possibility that the examined tumor type originates from transdifferentiation of partial HCC to iCCA, indicating the monoclonal origin of the tumor. This finding is supported by other current reports [6, 7], including our previous study [8] on mutation profiles of cHCC-CCA. We showed, using clinical

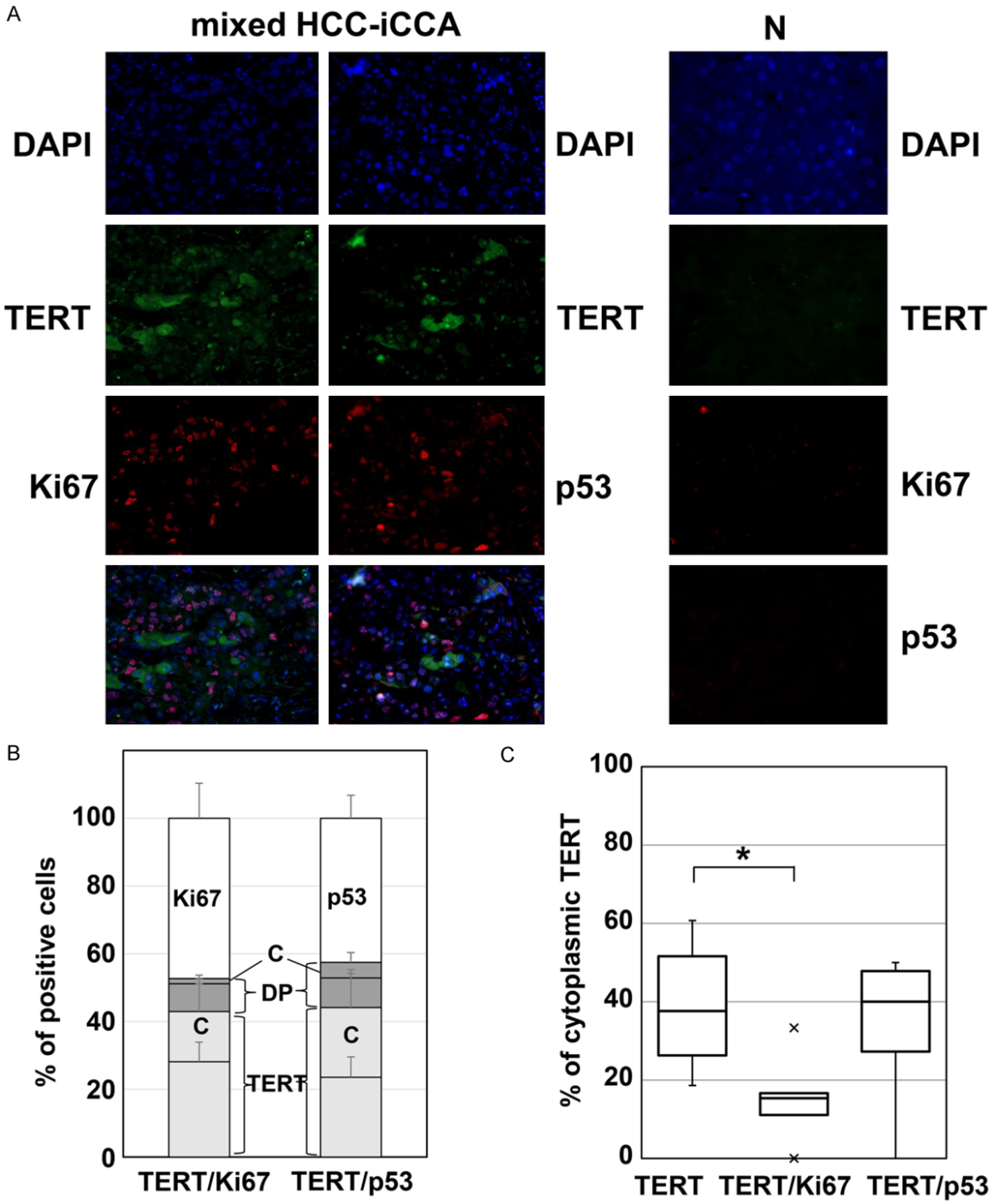

Figure 4. Immunofluorescence double staining of TERT/Ki67 and TERT/p53 proteins in the mixed HCC-iCCA component. A. Representative images of immunofluorescence double staining of TERT/Ki67 and TERT/p53. Cells positive for each protein were cancer cells in the mixed HCC-iCCA component (left panels). Representative images of three proteins in the noncancer region are shown on the right. B. Distributions of three types of cancer cell (TERT+, Ki67+, and TERT+/Ki67+) (TERT+, p53+, and TERT+/p53+) in two double-staining assays. The positive rate was determined in cancer cells. DP, double-positive cells (TERT+/Ki67+ and TERT+/p53+) shown in dark gray; C, cytoplasmic TERT-positive cells; single-positive cells for TERT+ shown in light gray and for Ki67+ or p53+ in white. C. Frequency of cytoplasmic TERT-positive cells among TERT+, TERT+/Ki67+, and TERT+/p53+ cancer cells. *, *P<0.05* by the Mann-Whitney *U* test.

samples, that the *TERT* promoter mutation C228T is actually related to TERT protein expression, especially through multiple cancer components of cHCC-CCA. However, the rate of

positivity was different in different cancer components, and not all cancer cells within a component were positive for the TERT protein (**Figure 3B**). For example, considering the frequency of *TERT* promoter mutation, 33.1%, in a tumor nodule of HCC+iCCA (**Figure 2A**), mutant cancer cells are estimated to compose 66.2% of total cells. Because mutant cancer cells are heterozygotes, the remaining cells are stromal cells without mutation. TERT protein positivity was detected in only 16.1±6.8% of cancer cells (**Figure 3B**) but not in all mutant cancer cells. This heterogeneity in TERT protein expression suggests that its expression is regulated by other factors; for example, TERT protein expression is more common in iCCA than in HCC (**Figure 3B**), suggesting a role for an iCCA-related factor. In general, overexpression of TERT in cancers is induced by a variety of mechanisms in addition to mutation of its promoter and may involve methylation, miRNA interference, and alternative splicing [9]. A more complicated mechanism is possibly involved in the observed heterogeneous expression of the TERT protein.

Cytoplasmic TERT expression was observed in the mixed HCC-iCCA component by immunofluorescence staining but not by IHC in this study, probably due to high reactivity of the secondary fluorescence antibody or high sensitivity of fluorescence acquisition. Although 16.1±6.8% of cancer cells were positive for TERT by IHC, 28.2±6.3% were positive for TERT (including 10.5±5.0% positive for cytoplasmic TERT) by immunofluorescence staining. Cytoplasmic TERT has also been observed in clinical samples of HCC, and this is the predominant site of TERT expression. Cytoplasmic TERT expression is associated with poor tumor differentiation and oxidative stress-related DNA damage [15]. In addition to the telomere-lengthening function (canonical function) of nuclear TERT, cytoplasmic TERT has many secondary telomere-independent roles (noncanonical functions), such as interaction with signaling pathways, stress protection, and binding to and protection of mitochondrial DNA [9]. Thus, the biologic function of cytoplasmic TERT remains to be elucidated; at least in our observation, Ki67-positive, actively proliferating cancer cells exhibited significantly less cytoplasmic TERT (**Figure 4C**). Ki67-positive cancer cells might prefer nuclear TERT with its canonical function; there seems to be a possible signaling linkage between cell proliferation and immortalization that involves telomere lengthening by nuclear translocation of TERT.

Second, we showed that the poor prognostic markers Ki67 and p53 were highly positive in iCCA; double-positive Ki67+/p53+ cells were also high-frequency compared to HCC (**Figure 3D** and **3E**). However, among Ki67-positive and p53-positive cancer cells of the mixed HCC-iCCA component, TERT+/Ki67+ and TERT+/p53+ cells were similar in relative frequency (**Figure 4B**). These results suggest that the iCCA component and iCCA-containing mixed component have a more malignant phenotype than the HCC component but that at the individual cell level, these malignant phenotypes are independently expressed. There are several IHC studies on Ki67 and p53 in HCC and iCCA cases but few on cHCC-CCA cases (Table S1). The mini-review of these data is described in comparison with ours (Supplementary Materials, Mini-review of the literature). Since there are few IHC studies on the quantitative comparison of a target protein among cancer components within a cHCC-CCA tumor, further investigation by use of multiple cHCC-CCA cases is necessary to confirm the higher positivity rate of the Ki67 and p53 proteins in the iCCA component versus the HCC component, and the correlation of these marker proteins at the individual cell level.

Third, we found unexpected expression of differentiation markers in some cancer components (**Figure 1B**, lower). These results also indicate heterogeneous development of cancer cells within homogenous HCC and iCCA components that are morphologically determined. For example, HCC cells within an HCC component were negative for both HepPar-1 and CK7 (**Figure 1B**, lower). Such double-negative HCC cells were observed in the HCC component in 4 of 9 cHCC-CCA cases (data not shown). A portion of HCC cells positive for HepPar-1 probably become dedifferentiated. The mechanism for this dedifferentiation is interesting, and it is unknown whether such dedifferentiation of HCC is a step of transdifferentiation toward iCCA. We also found iCCA cells positive for both CK7 and HepPar-1 scattered within an iCCA component (**Figure 1C**, lower). Such iCCA cells were observed in 3 of 6 cHCC-CCA cases (data not shown) and in other reports [16, 17]. Such simultaneously double-positive cells are typically observed in the 'intermediate cell carcinoma' of the 2019 WHO classification of cHCC-

CCA [1, 2]. However, double-positive iCCA cells in this study appear to be morphologically distinct from 'intermediate cell carcinoma' and are probably intermediate cells in transdifferentiation from HCC to iCCA. On the other hand, we found that the CA19-9-strongly positive cancer area consisted of three IHC-pattern regions: HepPar-1(+)/CK7(+), HepPar-1(+)/CK7(-), and HepPar-1(-)/CK7(+) regions (**Figure 1C**). These cancer regions morphologically corresponded to the mixture of HCC and iCCA, HCC and iCCA, respectively. Thus, CA19-9-positive, CK7-negative HCC cells were observed, but rarely, in cHCC-CCA (**Figure 1C**, high-magnification images). CA19-9 is aberrantly produced by gastrointestinal cancer cells, including biliary tract cancer cells. For HCC, dual-phenotype HCC (classical HCC expressing cholangiocyte markers) is strongly associated with the elevation of serum CA19-9 [18]. The CA19-9-positive HCC cells in our cHCC-CCA cases also represent an intermediate state in HCC to iCCA transdifferentiation.

To date, there have been few studies on the genetic and phenotypic characterization of individual cancer components within a given cHCC-CCA tumor, but such information is helpful for understanding the genesis and poor prognosis of this complex cancer. Recently, spatial omics and multiplexed imaging technologies have been developed to decipher cell-to-cell variation within and between individual tumors [19]. Trajectory inference approaches using single-cell transcriptome sequencing enable cells to be ordered within the lineage based on pseudotime [20]. These new technologies will drive future cancer biology research and aid in the development of diagnostic and therapeutic strategies for cHCC-CCA.

Acknowledgements

This work was supported in part by a grant from the Program for Promoting Advanced Medical Research in Nihon University School of Medicine, Tokyo, Japan (approval no. 2016). We thank Mr. Hiromu Naruse for his technical support regarding the dPCR of *TERT* promoter mutation.

Written informed consent was obtained from the patient.

Disclosure of conflict of interest

None.

Address correspondence to: Makoto Makishima and Mariko Esumi, Division of Biochemistry, Department of Biomedical Sciences, Nihon University School of Medicine, 30-1, Ohyaguchikami-cho, Itabashi-ku, Tokyo 173-8610, Japan. Tel: +81-3-3972-8111; E-mail: makishima.makoto@nihon-u.ac.jp (MM); esumi.mariko@nihon-u.ac.jp (ME)

References

[1] Sempoux C, Kakar S, Kondo F and Schirmacher P. Combined hepatocellular-cholangiocarcinoma and undifferentiated primary liver carcinoma. In: Bosman FT, Garneiro F, Hruban RH, Theise ND, editors. WHO Classification of Tumours of the Digestive System. Lyon: IARC; 2019. pp. 260-262.

[2] Beaufrere A, Calderaro J and Paradis V. Combined hepatocellular-cholangiocarcinoma: an update. J Hepatol 2021; 74: 1212-1224.

[3] Brunt E, Aishima S, Clavien PA, Fowler K, Goodman Z, Gores G, Gouw A, Kagen A, Klimstra D, Komuta M, Kondo F, Miksad R, Nakano M, Nakanuma Y, Ng I, Paradis V, Nyun Park Y, Quaglia A, Roncalli M, Roskams T, Sakamoto M, Saxena R, Sempoux C, Sirlin C, Stueck A, Thung S, Tsui WMS, Wang XW, Wee A, Yano H, Yeh M, Zen Y, Zucman-Rossi J and Theise N. cHCC-CCA: consensus terminology for primary liver carcinomas with both hepatocytic and cholangiocytic differentation. Hepatology 2018; 68: 113-126.

[4] Nagtegaal ID, Odze RD, Klimstra D, Paradis V, Rugge M, Schirmacher P, Washington KM, Carneiro F and Cree IA; WHO Classification of Tumours Editorial Board. The 2019 WHO classification of tumours of the digestive system. Histopathology 2020; 76: 182-188.

[5] Wang A, Wu L, Lin J, Han L, Bian J, Wu Y, Robson SC, Xue L, Ge Y, Sang X, Wang W and Zhao H. Whole-exome sequencing reveals the origin and evolution of hepato-cholangiocarcinoma. Nat Commun 2018; 9: 894.

[6] Joseph NM, Tsokos CG, Umetsu SE, Shain AH, Kelley RK, Onodera C, Bowman S, Talevich E, Ferrell LD, Kakar S and Krings G. Genomic profiling of combined hepatocellular-cholangiocarcinoma reveals similar genetics to hepatocellular carcinoma. J Pathol 2019; 248: 164-178.

[7] Xue R, Chen L, Zhang C, Fujita M, Li R, Yan SM, Ong CK, Liao X, Gao Q, Sasagawa S, Li Y, Wang J, Guo H, Huang QT, Zhong Q, Tan J, Qi L, Gong W, Hong Z, Li M, Zhao J, Peng T, Lu Y, Lim KHT, Boot A, Ono A, Chayama K, Zhang Z, Rozen SG, Teh BT, Wang XW, Nakagawa H, Zeng MS, Bai F and Zhang N. Genomic and transcriptomic profiling of combined hepatocellular and intrahepatic cholangiocarcinoma reveals distinct molecular subtypes. Cancer Cell 2019; 35: 932-947, e938.

[8] Ohni S, Yamaguchi H, Hirotani Y, Nakanishi Y, Midorikawa Y, Sugitani M, Naruse H, Nakayama T, Makishima M and Esumi M. Direct molecular evidence for both multicentric and monoclonal carcinogenesis followed by transdifferentiation from hepatocellular carcinoma to cholangiocarcinoma in a case of metachronous liver cancer. Oncol Lett 2022; 23: 22.

[9] Dratwa M, Wysoczanska B, Lacina P, Kubik T and Bogunia-Kubik K. TERT-regulation and roles in cancer formation. Front Immunol 2020; 11: 589929.

[10] Kawai-Kitahata F, Asahina Y, Tanaka S, Kakinuma S, Murakawa M, Nitta S, Watanabe T, Otani S, Taniguchi M, Goto F, Nagata H, Kaneko S, Tasaka-Fujita M, Nishimura-Sakurai Y, Azuma S, Itsui Y, Nakagawa M, Tanabe M, Takano S, Fukasawa M, Sakamoto M, Maekawa S, Enomoto N and Watanabe M. Comprehensive analyses of mutations and hepatitis B virus integration in hepatocellular carcinoma with clinicopathological features. J Gastroenterol 2016; 51: 473-486.

[11] Pezzuto F, Izzo F, De Luca P, Biffali E, Buonaguro L, Tatangelo F, Buonaguro FM and Tornesello ML. Clinical significance of telomerase reverse-transcriptase promoter mutations in hepatocellular carcinoma. Cancers (Basel) 2021; 13: 3771.

[12] Liu J, Li W, Deng M, Liu D, Ma Q and Feng X. Immunohistochemical determination of p53 protein overexpression for predicting p53 gene mutations in hepatocellular carcinoma: a meta-analysis. PLoS One 2016; 11: e0159636.

[13] Nault JC, Mallet M, Pilati C, Calderaro J, Bioulac-Sage P, Laurent C, Laurent A, Cherqui D, Balabaud C and Zucman-Rossi J. High frequency of telomerase reverse-transcriptase promoter somatic mutations in hepatocellular carcinoma and preneoplastic lesions. Nat Commun 2013; 4: 2218.

[14] Fujimoto A, Furuta M, Shiraishi Y, Gotoh K, Kawakami Y, Arihiro K, Nakamura T, Ueno M, Ariizumi S, Nguyen HH, Shigemizu D, Abe T, Boroevich KA, Nakano K, Sasaki A, Kitada R, Maejima K, Yamamoto Y, Tanaka H, Shibuya T, Shibata T, Ojima H, Shimada K, Hayami S, Shigekawa Y, Aikata H, Ohdan H, Marubashi S, Yamada T, Kubo M, Hirano S, Ishikawa O, Yamamoto M, Yamaue H, Chayama K, Miyano S, Tsunoda T and Nakagawa H. Whole-genome mutational landscape of liver cancers displaying biliary phenotype reveals hepatitis impact and molecular diversity. Nat Commun 2015; 6: 6120.

[15] Nishi Y, Aoki T, Shimizu T, Sato S, Matsumoto T, Shiraki T, Sakuraoka Y, Mori S, Iso Y, Ishizuka M and Kubota K. Significance of cytoplasmic expression of telomerase reverse transcriptase in patients with hepatocellular carcinoma undergoing liver resection. Mol Clin Oncol 2021; 15: 244.

[16] Terada T. Combined hepatocellular-cholangiocarcinoma with stem cell features, ductal plate malformation subtype: a case report and proposal of a new subtype. Int J Clin Exp Pathol 2013; 6: 737-748.

[17] Itoyama M, Hata M, Yamanegi K, Yamada N, Ohyama H, Hirano H, Terada N and Nakasho K. Expression of both hepatocellular carcinoma and cholangiocarcinoma phenotypes in hepatocellular carcinoma and cholangiocarcinoma components in combined hepatocellular and cholangiocarcinoma. Med Mol Morphol 2012; 45: 7-13.

[18] Lu XY, Xi T, Lau WY, Dong H, Zhu Z, Shen F, Wu MC and Cong WM. Hepatocellular carcinoma expressing cholangiocyte phenotype is a novel subtype with highly aggressive behavior. Ann Surg Oncol 2011; 18: 2210-2217.

[19] Lewis SM, Asselin-Labat ML, Nguyen Q, Berthelet J, Tan X, Wimmer VC, Merino D, Rogers KL and Naik SH. Spatial omics and multiplexed imaging to explore cancer biology. Nat Methods 2021; 18: 997-1012.

[20] Saelens W, Cannoodt R, Todorov H and Saeys Y. A comparison of single-cell trajectory inference methods. Nat Biotechnol 2019; 37: 547-554.

Supplementary Materials

Materials and methods

Liver specimens

The liver tumor from cHCC-CCA consisted of three components: HCC, iCCA and mixed HCC-iCCA (**Figure 1A**). Histologically, the HCC component displayed trabecular growth and was well differentiated (Edmondson and Steiner grade I [1]); the iCCA component was tubular and cord-like, with a fibrous stroma. The noncancer region had liver cirrhosis, with a fibrosis score of F4. Despite repeated treatment with transcatheter arterial chemoembolization against recurrent liver cancer six months later, the patient died a year after surgical resection.

DNA extraction

DNA was extracted from FFPE liver tissues prepared for pathological diagnosis. Multiple cancer and noncancer regions of the FFPE thin sections were separately macrodissected or microdissected using laser capture microdissection techniques. Regarding dissection of the cancer region (HCC+iCCA) and noncancer region (N), 10-μm-thick FFPE sections were mounted onto cleaned glass slides, and the target regions were scraped off using the glass slide edge after dewaxing. DNA was extracted as described previously [2]. For laser capture microdissection, 8-μm-thick FFPE tissue sections were mounted onto membrane film-coated glass slides (Zeiss, Oberkochen, Germany). Following dewaxing with xylene and ethanol, the sections were stained with toluidine blue, and the target regions of HCC, CCA, and mixed HCC-iCCA were microdissected using PALM MB-IV (Zeiss). The microdissected samples were lysed in DNA lysis buffer that contained 2% sodium dodecyl sulfate, 0.1 mM ethylenediaminetetraacetic acid and 10 mM tris-hydrochloride and incubated overnight at 55°C with proteinase K (QIAGEN N. V., Hilden, Germany). DNA was extracted with buffer-saturated phenol (pH 8.0)-chloroform-isoamyl alcohol (25:24:1), followed by precipitation with ethanol.

Digital polymerase chain reaction (dPCR) of the TERT promoter mutation C228T

The TERT promoter mutation C228T was assessed as described previously [2] using TaqMan dPCR Liquid Biopsy Assay TERT_C228T (Hs000000092_rm, Thermo Fisher Scientific, Waltham, MA, USA) with a QuantStudio 3D Digital PCR System (Thermo Fisher Scientific). The dPCR data were analyzed using QuantStudio 3D AnalysisSuite version 3.1 (Thermo Fisher Scientific). Reproducibility and negative controls were confirmed as described previously [2].

Immunohistochemistry

Serial thin sections (4 μm) of FFPE tissues were subjected to IHC for hepatocyte paraffin (HepPar)-1, cytokeratin (CK)7, CK19, carbohydrate/cancer antigen (CA)19-9, TERT, Ki67 and p53. IHC was performed basically as described previously [2]. Antigen retrieval was performed using 10 mM citrate buffer (pH 6.0) at 105°C for 10 min for CK7, CK19 and CA19-9; 10 mM citrate buffer (pH 9.0) at 105°C for 10 min for HepPar-1, Ki67 and p53; and 10 mM citrate buffer (pH 9.0) at 100°C for 20 min for TERT. The primary antibodies used were as follows: mouse monoclonal anti-human hepatocyte (HepPar-1) antibody (1:100, clone OCH1E5, code M7158, Agilent Technologies, Santa Clara, CA, USA), mouse monoclonal anti-CK7 antibody (1:100, clone OV-TL 12/30, code M7018, Agilent Technologies), mouse monoclonal anti-CK19 antibody (1:80, clone RCK108, code M0888, Agilent Technologies), mouse monoclonal anti-CA19-9 antibody (1:50, clone 1116-NS-19-9, code M3517, Agilent Technologies), mouse monoclonal anti-TERT antibody (1:50, clone A-6, code sc-393013, Santa Cruz Biotechnology, Santa Cruz, CA, USA), mouse monoclonal anti-Ki67 (1:50, clone MIB-1, code M7240, Agilent Technologies) and mouse monoclonal anti-p53 (1:50, clone DO7, code M7001, Agilent Technologies). After incubation with the primary antibody for 30 min at room temperature, the sections were incubated with Histofine Simple Stain MAX-PO (MULTI, Nichirei Bioscience) as the secondary antibody for 30 min at room temperature, visualized with 3,3'-diaminobenzidine chromogen (Wako Pure Chemical Industries, Osaka, Japan) and counterstained with hematoxylin.

For IHC for TERT, Ki67 and p53, the proportion of antigen-positive cells was determined in each component of cancer and noncancer regions. The numbers of antigen-positive cancer cells and total cancer cells were measured in ten fields of each histological component using cellSens Dimension 1.16 (Olympus, Tokyo, Japan). Similarly, the numbers of hepatocytes were measured in noncancer regions. The positive rate was obtained from each of 10 fields and is expressed as a box plot and statistically compared among histologic components using the Mann-Whitney U test. IHC for Ki67 and p53 in serial sections was also used to identify double-positive (Ki67+/p53+) cancer cells. The number of Ki67-positive or p53-positive cancer cells was determined in the same field of serial sections, and that of double-positive cancer cells was also determined by comparing these two IHC images. The number of single-positive cancer cells was calculated by subtracting the above values. Five fields of each component of cancer were subjected to measurement. The distribution of Ki67+, p53+, and Ki67+/p53+ cells was compared among cancer components using the chi-square test.

Immunofluorescence double staining for TERT/Ki67 and TERT/p53

Thin sections of FFPE tissues (4 μm) were subjected to antigen retrieval in the same way as IHC for TERT, Ki67, and p53. After blocking with normal goat serum for 10 min, the sections were incubated with two primary antibodies, mouse anti-TERT antibody (1:50, clone A-6, code sc-393013, Santa Cruz Biotechnology) and rabbit monoclonal anti-Ki67 antibody (ready to use, clone SP6, code 418071, Nichirei Bioscience) or rabbit monoclonal anti-p53 (1:2000, clone EPR17343, code ab179477, Abcam, Cambridge, UK), for 1 h at room temperature. The sections were then incubated with Alexa Fluor 488-labeled anti-mouse (1:500, ab150117, Abcam) or Alexa Fluor 594-labeled anti-rabbit (1:500, A11072, Thermo Fisher Scientific) secondary antibodies for 30 min at room temperature. The sections were mounted with Diamond Antifade Mountant with DAPI (4',6-diamidino-2-phenylindole) (Thermo Fisher Scientific). Fluorescence images were acquired with an Axio Imager Z2 Upright Microscope (Carl Zeiss, Oberkochen, Germany) and ZEN 2 Pro software (Carl Zeiss). The total cell number was determined by counting DAPI-stained cancer nuclei, and the numbers of single-positive cancer cells for TERT (TERT+) and Ki67 (Ki67+) and double-positive cancer cells for TERT and Ki67 (TERT+/Ki67+) were also counted in each of five fields from the TERT/Ki67 double staining. The same cell counting procedure was performed for TERT/p53 double staining. The distribution of single-positive and double-positive cancer cells was determined in the mixed HCC-iCCA region for TERT/Ki67 and TERT/p53 double staining. The distribution of three types of cancer cells was compared between the two double-staining methods using the chi-square test. Cytoplasmic staining for TERT was also assessed in five fields each for the two double-staining methods. The frequency of cytoplasmic TERT-positive cells was compared statistically among three types of cancer cells (TERT+, TERT+/Ki67+, and TERT+/p53+) using the Kruskal-Wallis test.

Statistical analysis

Statistical analysis was performed using the Mann-Whitney U test for the positive rate of TERT, Ki67 and p53 immunohistochemistry among HCC:iCCA, iCCA:HCC (#3), and HCC:HCC (#3). The distribution of three types of cancer cells (Ki67+, p53+, Ki67+/p53+) between HCC and iCCA was statistically analyzed using the chi-square test. Additionally, the distribution of three types of cancer cells (TERT+, Ki67+, or p53+, TERT+/Ki67+ or TERT+/p53+) between TERT/Ki67- and TERT/p53 double-staining experiments was analyzed using the chi-square test. The positive rate of cytoplasmic TERT among TERT+, TERT+/Ki67+, and TERT+/p53+ cells was analyzed using the Kruskal-Wallis test. A p value < 0.05 was considered significant.

References

[1] Edmondson HA and Steiner PE. Primary carcinoma of the liver: a study of 100 cases among 48,900 necropsies. Cancer 1954; 7: 462-503.

[2] Ohni S, Yamaguchi H, Hirotani Y, Nakanishi Y, Midorikawa Y, Sugitani M, Naruse H, Nakayama T, Makishima M and Esumi M. Direct molecular evidence for both multicentric and monoclonal carcinogenesis followed by transdifferentiation from hepatocellular carcinoma to cholangiocarcinoma in a case of metachronous liver cancer. Oncol Lett 2022; 23: 22.

Mini-review of the literature: IHC studies on Ki67 and p53 in liver cancers

There are several IHC studies on Ki67 and p53 in HCC [2-6] and iCCA [7-12] cases but few in cHCC-CCA cases [1]. Table S1 shows the comparative review of these data, including ours. For most cases, p53 overexpression is significantly related to proliferative activity, as evaluated by the Ki-67 labeling index [3-5, 8]. For rare cases, the quantitative comparison using the labeling index for both Ki67 and p53 also indicates a significant correlation [3, 4]. The labeling indices for Ki-67 and p53 varied with tumor grade and differed in individual reports. Our data of multiple cancer components even from a single case seem to be reasonable, supported by the similar results of a component study in cHCC-CCA [1] and a similar labeling index of the two markers shown in individual cancers [2-4]. However, there is no report in which double-positive Ki67+/p53+ cells were quantitatively examined at the individual-cell level, as in our study.

Table S1. IHC studies on Ki67 and p53 in liver cancers

Liver cancer	Case No.	Subgroup	Positive cell (%)		Positive case (%)	Ref No.
			Ki67	p53	p53	
cHCC-CCA	1* (10)	HCC comp (#2b)	12.0±2.7	12.7±3.6		Our study
		HCC comp (#3)	13.9±9.6	16.1±8.4		
		iCCA comp (#2b)	32.0±8.2	34.7±8.3		
cHCC-CCA	14	HCC component	4.4±3.4		4 (22%)	[1]
		iCCA component	11.0±8.5		5 (29%)	
HCC	11		3.9±2.2			
iCCA	8		12.7±5.6			
HCC	29	Total***	16.3±11.1	10.5±15.0		[2]
	11** (25)	Total	10.2±12.8	13.2±19.0 (r=0.865)	9 (36%)	[3]
		p53(+) (9)	24.0±12.0			
		p53(-) (16)	2.5±2.9			
	35	Total	29.7±22.9	28.8±24.7 (r=0.416)	27 (77%)	[4]
		p53(+) (27)	37.0±20.5			
		p53(-) (8)	5.0±4.6			
	50	Total	13.6±7.3		15 (30%)	[5]
		p53(+) (15)	23.3±6.0			
		p53(-) (35)	9.4±1.8			
	57	Total	18.6±12.2		30 (53%)	[6]
iCCA	26	Total	22.9 (4.1-56.6)	14.6 (0.2-69.9)		[7]
	41	Total	28.9±26.1		13 (32%)	[8]
		p53(+) (13)	40.2±23.1			
		p53(-) (28)	23.7±26.1			
	23	Total	23.0±5.9		7 (30%)	[9]
		p53(+) (7)	30.0±3.2			
		p53(-) (16)	19.9±3.8			
	47	Total	19.6±13.2		27 (57%)	[10, 11]
	28	Total	20.1±6.9		10 (36%)	[12]

*Ten microscopic fields of each cancer component were examined for Ki67 and p53. **Each of 11 HCC cases contains more than two histological grades, and a total of 25 areas were examined for Ki67 and p53. ***Total percentage of positive cells was calculated by integrating data shown in the reference. The correlation coefficient (r) of Ki67 and p53 was calculated from raw data of the percentage of positive cells. Square brackets indicate statistically significant differences. Ref, reference.

References

[1] Wakasa T, Wakasa K, Shutou T, Hai S, Kubo S, Hirohashi K, Umeshita K and Monden M. A histopathological study on combined hepatocellular and cholangiocarcinoma: cholangiocarcinoma component is originated from hepatocellular carcinoma. Hepatogastroenterology 2007; 54: 508-513.

[2] Yamagami T, Shibata M, Ueno Y, Watanabe M and Terauch I. [title in Japanese]. Kanzo 1993; 34: 1009-1010.
[3] An FQ, Matsuda M, Fujii H, Tang RF, Amemiya H, Dai YM and Matsumoto Y. Tumor heterogeneity in small hepatocellular carcinoma: analysis of tumor cell proliferation, expression and mutation of p53 and beta-catenin. Int J Cancer 2001; 93: 468-474.
[4] Anzola M, Saiz A, Cuevas N, Lopez-Martinez M, Martinez de Pancorbo MA and Burgos JJ. High levels of p53 protein expression do not correlate with p53 mutations in hepatocellular carcinoma. J Viral Hepat 2004; 11: 502-510.
[5] Nagao T, Kondo F, Sato T, Nagato Y and Kondo Y. Immunohistochemical detection of Aberrant p53 expression in hepatocellular carcinoma: correlation with cell proliferative activity indices, including mitotic index and MIB-1 immunostaining. Hum Pathol 1995; 26: 326-333.
[6] Koskinas J, Petraki K, Kavantzas N, Rapti I, Kountouras D and Hadziyannis S. Hepatic expression of the proliferative marker Ki-67 and p53 protein in HBV or HCV cirrhosis in relation to dysplastic liver cell changes and hepatocellular carcinoma. J Viral Hepat 2005; 12: 635-641.
[7] Tsokos CG, Krings G, Yilmaz F, Ferrell LD and Gill RM. Proliferative index facilitates distinction between benign biliary lesions and intrahepatic cholangiocarcinoma. Hum Pathol 2016; 57: 61-67.
[8] Ito Y, Takeda T, Sasaki Y, Sakon M, Yamada T, Ishiguro S, Imaoka S, Tsujimoto M and Matsuura N. Expression and clinical significance of the G1-S modulators in intrahepatic cholangiocellular carcinoma. Oncology 2001; 60: 242-251.
[9] Jarnagin WR, Klimstra DS, Hezel M, Gonen M, Fong Y, Roggin K, Cymes K, DeMatteo RP, D'Angelica M, Blumgart LH and Singh B. Differential cell cycle-regulatory protein expression in biliary tract adenocarcinoma: correlation with anatomic site, pathologic variables, and clinical outcome. J Clin Oncol 2006; 24: 1152-1160.
[10] Ashida K, Terada T, Kitamura Y and Kaibara N. Expression of E-cadherin, alpha-catenin, beta-catenin, and CD44 (standard and variant isoforms) in human cholangiocarcinoma: an immunohistochemical study. Hepatology 1998; 27: 974-982.
[11] Horie S, Endo K, Kawasaki H and Terada T. Overexpression of MDM2 protein in intrahepatic cholangiocarcinoma: relationship with p53 overexpression, Ki-67 labeling, and clinicopathological features. Virchows Arch 2000; 437: 25-30.
[12] Kim HJ, Yun SS, Jung KH, Kwun WH and Choi JH. Intrahepatic cholangiocarcinoma in Korea. J Hepatobiliary Pancreat Surg 1999; 6: 142-148.